Acta Cryst. (1995). B51, 1016–1020

Solids Modelled by Crystal Field *Ab Initio* Methods. IX.* Stereoselective Order–Disorder in Tri-*ortho*-thymotide–3-Buten-2-ol (2/1) Clathrate

BY K. VERHULST, A. T. H. LENSTRA AND C. VAN ALSENOY

University of Antwerp (UIA), Department of Chemistry, Universiteitsplein 1, *B*-2610 *Wilrijk, Belgium*

(*Received* 27 *May* 1994; *accepted* 10 *March* 1995)

Abstract

Geometries of 3-buten-2-ol (CH_3—CHOH—CH=CH_2) were optimized using standard *ab initio* SCF–LCAO–MO methods, as well as the electrostatic crystal field (ECF–MO) approach. Comparisons are made between isolated butenol molecules and molecules packed in a tri-*ortho*-thymotide (TOT) clathrate, 1,7,13-trimethyl-4,10,16-tris(1-methylethyl)-6*H*,12*H*,18*H*-tribenzo[*b*,*f*,*j*][1,5,9]trioxacyclododecin-6,12,18-trione. Excellent agreement is obtained with available microwave and diffraction data. Despite the neglect of orbital overlap between neighbouring molecules, all the significant geometric differences between the gas phase and the solid state are well reproduced. Specifically we note the differences in C=C—C—O torsion angles. The presence of both *R* and *S* configurations in the TOT-clathrate with a low degree of chiral discrimination has been experimentally verified. From the difference in calculated molecular energy between the two butenol enantiomers that were optimized within the TOT-clathrate, the observed enantiomeric excess of 4–6% in favour of (*R*)-butenol is reproduced.

Introduction

When biological systems interact with racemic substrates they often display an extraordinarily high degree of chiral discrimination. The inclusion complexes of tri-*ortho*-thymotide (TOT, Fig. 1) provide a possible medium for reactions of included guest molecules and present an interesting system for studying these host–guest interactions (Gerdil & Allemand, 1980). TOT is a switchable molecule (Rogers, 1975); the molecule can easily change its configuration from image to mirror image by rotations about the carboxylic bonds. In its pure form an equilibrium solution of TOT molecules crystallizes in the racemic space group $Pna2_1$. The ease by which a molecule goes from one enantiomeric form to the other depends on the height of the rotation barrier. Another well known example of switchable behaviour is biphenyl (Lenstra, Van Alsenoy, Verhulst & Geise, 1994). In the gas phase the barrier height for rotation around the central C—C bond is *ca* 1.9 kcal mol^{-1} (7.95 kJ mol^{-1}). Hence, a racemic mixture of non-switchable molecules typifies the gaseous state. However, in solution and in the solid state the near-neighbour interactions lower the rotation barrier to 0.8 kcal mol^{-1} (3.35 kJ mol^{-1}) and thus biphenyl acts as a switchable molecule in the liquid and solid state. Lowering the thermal energy by cooling the biphenyl crystal below 40 K leads to a series of phase transitions which reflect an order–disorder competition between the optical antipodes of biphenyl. This suffices to show the importance of intermolecular interactions when we deal with switchable molecules.

In contrast to biphenyl TOT has the ability to form clathrates with a wide variety of guest molecules. Crystallization of TOT from solutions of appropriate racemic guest compounds yields chiral single crystals of clathrate complexes in which the guest enantiomers are incorporated to different degrees. This chiral discrimination towards the guest molecules leads to order–disorder problems in the clathrate crystal lattice. Channel-type complexes (space group $P6_1$) or cage-type complexes (space group $P3_121$) are obtained. Especially in the cage-type complexes the enantiomeric excess of the guest molecule varies widely, while this excess is rather low in the channel-type complexes (Table 1). It has been proved that chiral discrimination is caused by intermolecular interactions in the crystal. Therefore, the crystal structures define the discriminating interactions between the TOT molecules and the more and less favoured guest enantiomers (Arad-Yellin, Green, Knossow & Tsoucaris, 1983). The purpose of this work is to investigate the features that control these chiral interactions *via* electrostatic crystal field perturbed molecular orbital (ECF–MO) calculations on TOT-3-buten-2-ol (2/1) clathrate (Siripitayananon & Gerdil, 1989).

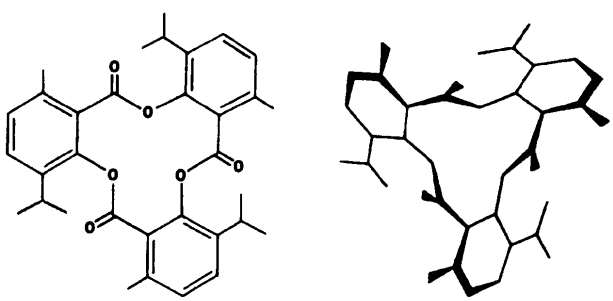

Fig. 1. Geometry and idealized view of a tri-*ortho*-thymotide molecule.

* Part 8: Peeters, Van Alsenoy, Lenstra & Geise (1994).

Table 1. *Enantiomeric excess (in percentages) of guest molecules in TOT clathrate crystals (Arad-Yellin, Green, Knossow & Tsoucaris, 1983)*

Guest molecule	Clathrate type	Enantiomeric excess	Guest configuration
2-Bromobutane	Cage	37	*S*
2-Chlorobutane	Cage	32	*S*
Methyl-methanesulfinate	Cage	14	*R*
2-Bromononane	Channel	5	*S*
2-Chlorooctane	Channel	4	*S*

Table 2. *Theoretical and experimental geometries of isolated (R)-butenol rotamers*

	Theoretical			
	Rot. 1	Rot. 2	Rot.3	Experimental
C1—H1–3	1.115	1.115	1.115	1.093 ass.
C1—C2	1.535	1.532	1.528	1.528 ass.
C2—H4	1.120	1.118	1.120	1.093 ass.
C2—O1	1.428	1.434	1.436	1.415 ass.
O1—H5	0.964	0.964	0.964	0.969 ass.
C2—C3	1.517	1.512	1.518	1.496 ass.
C3—H6	1.109	1.109	1.111	1.090 ass.
C3=C4	1.339	1.340	1.339	1.331 ass.
C4—H7,8	1.106	1.108	1.106	1.090 ass.
C1—C2—O1	105.5	104.9	105.0	112.3 ass.
C1—C2—C3	111.6	112.1	115.0	112.3 110.3
C3—C2—O1	111.7	110.0	110.1	112.3 ass.
C2—C3=C4	123.8	124.3	126.6	126.8 126.8
C=C—C—C	−103.8	116.8	13.6	−124 118
C=C—C—O	14.0	−126.8	131.9	4 −122
$E_{mol.}$	−605 460.7	−605 459.1	−605 446.4	
$E_{rel.}$	0.00	1.7	14.2	

Bond lengths are in Å, valence angles and torsions are in °. The calculated r_e(4–21 G) distances were transformed into r_g(calc) distances using: $r_g(\text{calc}) = r_e(4\text{–}21\,\text{G}) + \delta$ with δ(C—O) = −0.023, δ(C—C) = −0.008, δ(C=C) = +0.026, δ(C—H) = +0.034 and δ(O—H) = 0.000 Å. Experimental bond lengths and some valence angles were assumed in order to fit the different rotational constants. The other parameters were adjusted for the two favourable rotamers (Smith, Carballo, Bright Wilson, Marstokk & Møllendal, 1985). The molecular and relative energies are in kJ mol.$^{-1}$

Geometry of an isolated butenol molecule

In order to analyse the importance of surrounding molecules on the molecular geometry, we first optimized the geometry of an isolated (*R*)-butenol molecule using Pulay's gradient method, the computer program *BRABO* (Van Alsenoy, 1988; Van Alsenoy & Peeters, 1993) and the 4–21 G basis set (Pulay, Fogarasi, Pang & Boggs, 1979). The relaxation was considered complete when the residual forces on the separate atoms were smaller than 10 pN. At this level of refinement it is believed that the bond lengths are within 0.0005 Å and the valence angles are within 0.2° from their 4–21 G optimum value.

Three equilibrium geometries for an isolated butenol molecule were obtained. The differences in bond lengths and valence angles are not significant, the three conformers only differ in C=C—C—O torsion angle. The final results of all three gas phase refinements as well as the experimental geometries for the butenol rotamers are given in Table 2, the atoms being numbered as in Fig. 2. The butenol rotamer with a C=C—C—O torsion of 14.0° (Rot. 1) has the lowest energy. The energy of the conformation with a torsion of −126.8° (Rot. 2), however, is only *ca* 1.7 kJ mol^{-1} higher. The quasi 50/50 presence of these two butenol rotamers in the gas phase is experimentally verified by a microwave analysis (Smith, Carballo, Bright Wilson, Marstokk & Møllendal, 1985). The relatively much higher energy of the third rotamer (Rot. 3) explains why this conformation is not experimentally observed. We also calculated the C=C—C—O torsion potential for an isolated butenol molecule, keeping the rest of the refined geometry fixed. The barrier to rotation is illustrated in Fig. 3.

A search within the Cambridge Structural Database (CSD; Allen, Kennard & Taylor, 1983) was performed in order to discover geometrical trends in analogous products concerning the value of the C=C—C—O torsion angle. The structural unit that was submitted is depicted in Fig. 4. The search yielded 272 hits in 74 different molecules. The accessory histogram, plotted in Fig. 5, shows the distribution of the 272 hits as a function of the C=C—C—O torsion angle. Remarkably enough, the frequency distribution of this torsion angle in the solid state does not match the torsional energy profile calculated for an isolated molecule. This makes it abundantly clear that the butenol moiety easily adjusts its own geometry in the solid state under the influence of

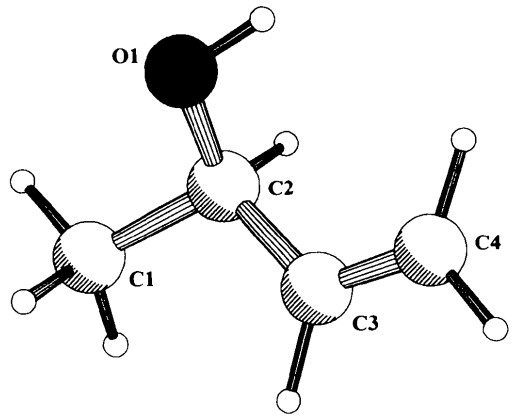

Fig. 2. The atomic numbering scheme of (*R*)-3-buten-2-ol.

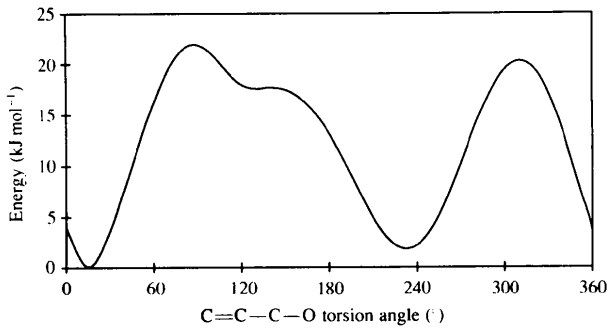

Fig. 3. Barrier to rotation for an isolated butenol molecule.

nearest-neighbour interactions. An increase in its own molecular energy by 5 kcal mol^{-1} (20.934 kJ mol^{-1}) is not really exceptional. The two butenol entities observed in the TOT-clathrate (see Gerdil & Allemand, 1980) show torsion angles that are among the most populated ones in the CSD inferred histogram.

Crystal field solid-state modelling

It is possible to introduce the effect of surrounding molecules on a central molecule within a crystal structure into *ab initio* calculations by using a crystal field approach (Popelier, Lenstra, Van Alsenoy & Geise, 1989, 1991). When the intermolecular distances within the crystal lattice are larger than van der Waals distances only the central molecule, in this case the butenol molecule, is described by its wavefunction. The neighbouring molecules within a radius of *ca* 10 Å are represented by Mulliken point charges, one per atomic position. These point charges generate an electrostatic field which is superimposed as a perturbation on the molecular wavefunction. The lattice energy of an ionic crystal structure is given by (Ketelaar, 1958)

$$U = -N\alpha e^2/r,$$

where α is the Madelung constant. In the case of a lattice such as that of NaCl, the Madelung constant is $\alpha = 1.7476$. Splitting the lattice in shells of near neighbours the electrostatic potential follows the expression

$$V = -6e/r + 12e/r2^{1/2} - 8e/r3^{1/2} + 6e/2r \ldots$$

This lattice sum converges very slowly. The absence of rapid convergence in the electrostatic potential is frequently used to criticize our 'cluster' approach. A coordinating layer with a thickness of 10 Å in which the wave-functional behaviour is analysed cannot lead to an electrostatic perturbation in line with the real crystalline potential unless we are very lucky. This criticism is correct when one wants to obtain a proper estimate for the lattice energy. We use this crystal field approach, however, primarily to obtain an equilibrium geometry for the crystalline state because molecular geometry adjustments to local situations (*e.g.* gas-phase structure *versus* solid-state structure) reflect the impact of intermolecular interactions. In our model the driving force behind the molecular response to packing forces is dictated by Coulomb interactions. Therefore, the outcome is determined by dV/dr and not by V. Since the series for this potential gradient is a function of $1/r^2$, it converges more rapidly than the electrostatic potential. This suggests that our cluster model is capable of producing an adequately converged 'solid-state' equilibrium geometry.

The lattice energy that follows from the cluster calculations is not by definition a sample without value. Especially when one deals with electrically neutral clusters this energy estimate is often a useful indicator for the lattice energy itself. This correspondence was essential in our biphenyl analysis (Lenstra, Van Alsenoy, Verhulst & Geise, 1994). To illustrate our point, we briefly report the results of a geometry optimization of cubic acetylene (space group $Pa3$). We chose this structure because experimental evidence exists to verify this approach (Kihara, 1960). When linear quadrupoles constructed of magnets [q $-q$ $-q$ q] are allowed to assemble themselves into a lattice, they were found to 'crystallize' in the cubic space group $Pa3$. We refined the geometry of the central molecule within clusters of point charges with a radius varying from 0 (gas phase) up to 20 Å. We also looked at the convergence of what can be regarded as the lattice energy (*i.e.* the energy of the total cluster diminished with the electrostatic contribution) as a function of the cluster size. Both aspects of these calculations are illustrated in Fig. 6. It is clear that both the molecular geometry as well as the molecular energy are converged to an equilibrium when the radius of the cluster is 8 Å or more.

The rapid convergence of the lattice energy is in our view not typical for acetylene alone. It is also found in

Fig. 4. Search unit for the CSD system.

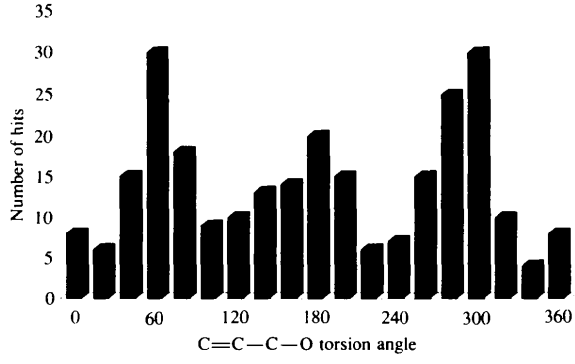

Fig. 5. Histogram for the structural fragment.

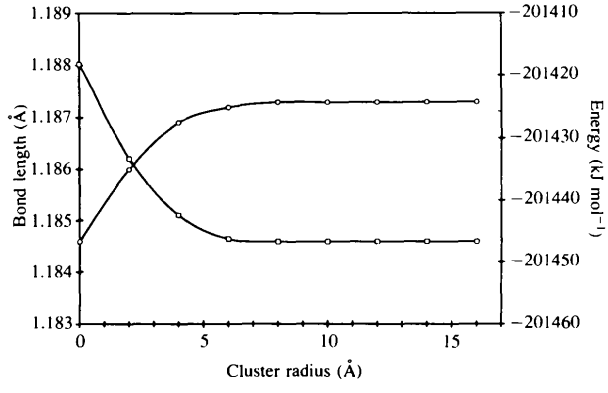

Fig. 6. C≡C bond length (o) and lattice energy (□) *versus* cluster size.

the ionic structure of NaCl. In the potential series given above one ignores the fact that crystals are electrically neutral. The incorporation of this boundary condition in the calculation of the Madelung constant leads to a serious suppression of the oscillation of the Madelung constant. 48 neighbouring shells are required to produce for the first time a neutral coordination around the reference ion. At this point the NaCl cluster has a radius of *ca* 20 Å. The cluster energy produces a pseudo-Madelung value of 0.9 × its ideal value. Remarkably enough, this cluster energy is an almost perfect representation of the true lattice energy of NaCl which – when the Born repulsion was included in our lattice energy expression – reduces to

$$U = -N\alpha e^2/r(1 - 1/n), \text{ with } n = 9.$$

Both examples, acetylene and NaCl, are in our opinion sufficient to illustrate that it would be unwise to ignore available lattice energy estimates. Only when the experimental evidence contradicts the cluster energy-inferred structure properties is it time to accept the shortcomings of our electrostatic crystal field perturbed calculations.

Geometry optimization

In the case of TOT/butenol (2/1) we constructed a cluster of seven TOT molecules that were within a 10 Å range from the butenol molecule to be optimized. The experimental TOT coordinates were used and kept fixed during the relaxation procedure. The equivalent positions of the seven TOT units that form the cavity in which the butenol molecule resides are listed in Table 3. The shortest intermolecular distances between the butenol molecule and its surrounding cage are 2.74 and 3.31 Å for a H and non-H atom, respectively, *i.e.* larger than the appropriate van der Waals distances.

The overall shape of the potential profile within the TOT cavity is dictated by the largest terms in the V series. Large charges are more important than small ones when these charges are located at similar distances from the cavity. Chemistry is traditionally a configurational science, *i.e.* it is severely biased to group properties. Within the TOT molecule two important groups can be distinguished, *viz.* the benzene moieties and the carboxyl groups. The latter are polar and as a consequence will dominate the potential within the cavity. From a Mulliken population analysis on formic acid we estimated charges of +0.5e for the C atoms and −0.5e for the O atoms. In this way we assemble a cluster of carboxyl groups with an overall charge of −10.5e. Using all the benzene fragments as slave units, their 210 C atoms must each have a charge of +0.05e in order to preserve an electrically neutral cluster. Superimposing the approximation of the real electrostatic potential as a perturbation on the wavefunction, we started the geometry optimization of the butenol conformations.

Table 3. *The seven TOT molecules that construct the butenol cage (space group $P3_121$)*

TOT	Equivalent position		
1	x	y	z
2	$x-1$	$y-1$	z
3	$y-1$	x	$-z$
4	x	$y-1$	z
5	$-x$	$y-x$	$\frac{1}{3}-z$
6	$1-x$	$y-x$	$\frac{1}{3}-z$
7	$1-y$	$x-y+1$	$\frac{1}{3}+z$

Table 4. *Experimental and theoretical butenol geometries within the TOT-clathrate*

	R configuration		*S* configuration	
	Experimental	Theoretical	Experimental	Theoretical
C1—H1-3	1.116	1.116	1.113	1.117
C1—C2	1.535	1.520	1.537	1.519
C2—H4	1.115	1.118	1.121	1.119
C2—O1	1.418	1.445	1.416	1.444
O1—H5	0.943	0.963	0.941	0.963
C2—C3	1.515	1.515	1.511	1.515
C3—H6	1.103	1.107	1.104	1.107
C3=C4	1.338	1.339	1.338	1.339
C4—H7,8	1.102	1.109	1.102	1.108
C=C—C—C	−171.6	−167.9	171.5	169.5
C=C—C—O	−50.2	−48.0	49.8	50.3
$E_{rel.}$ with electrostatic contribution		0.00		5267.83
$E_{rel.}$ molecular		0.00		155.33

Bond lengths are in Å, torsion angles in (°). The data depicted concerning the experimental geometries were calculated from the crystallographic coordinates reported by Gerdil & Allemand (1980). The relative energies are in J mol^{-1}.

The relaxations were considered to be converged when the largest residual force on a separate atom was smaller than 15 pN. Whether we optimized the butenol molecule within the electrostatic cluster in its neutral form or we refined the butenol geometry in a field generated by the carboxyl groups alone, we arrived at almost identical equilibrium geometries. In fact, the two final geometries can be regarded as equal within the geometrical error margins dictated by our convergence criterion for residual forces. Therefore, an incomplete-field model based upon chemical intuition or a more complete model respecting electroneutrality are both acceptable when judged by the final butenol geometry.

The results concerning the refinements of both the *R* and *S* conformer in a fixed TOT environment within the functional group biased logic are listed in Table 4. After convergence in the 4–21 G basis set structured computations the C=C—C—C torsion angle of the (*R*)-butenol was −167.9°, *i.e.* deviating only by 3.7° from the X-ray crystallographic value of −171.6°. The same torsion within the (*S*)-butenol was 169.5°, only 2.0° different from the experimental value. The solid-state model also yielded C=C—C—O torsions of −48.0 and 50.3° for the *R* and *S* conformers, respectively, which deviate only 2.2 and 0.5° from the experimental C=C—C—O torsions of −50.2 and 49.8°. These geometrical results are surprisingly good considering the simplifications introduced into the electrostatic 'cage' model.

Energetic considerations

The host–guest interactions between TOT and butenol molecules can be expressed by the difference in lattice energy of the clathrates accommodating the *R* and *S* configurations, respectively. For this particular case semi-empirical lattice energies calculated from molecular modelling are reported that favour the TOT–(*R*)-butenol interaction by 1.1 kcal mol^{-1} (4.61 kJ mol^{-1}) with and by 0.6 kcal mol^{-1} (2.51 kJ mol^{-1}) without optimization of the cell parameters (Siripitayananon & Gerdil, 1989). Our electrostatic crystal-field perturbed *ab initio* results produce a cluster energy difference of 1.3 kcal mol^{-1} (5.44 kJ mol^{-1}) in favour of the TOT–(*R*)-butenol interaction. This is very much in line with the semi-empirical results mentioned. These estimated energy differences, however, have a practical consequence, *viz.* an almost zero presence of (*S*)-butenol in the TOT lattice. Siripitayananon *et al.* have found from the amplitude of optical rotations an enantiomeric excess in favour of (*R*)-butenol of only 4–6%. Thus, tested against the reality in the solid state we have to conclude that the obtained lattice energies – semi-empirical and *ab initio* – are unsatisfactory.

With cluster energies too inaccurate to be useful we decided to return to the most reliable result, namely the solid-state adjusted butenol geometries. Keeping these crystalline geometries fixed, the geometrical impact of the nearest-neighbouring molecules on the butenol molecules is easily preserved. With this concept we calculated on a molecular basis an energy difference between the (*R*)- and (*S*)-butenol molecules of 155.33 J mol^{-1}. Using the classical Boltzmann partition function $\exp(-E_i/RT)$, this improved energy difference estimate leads at room temperature to an enantiomeric excess of (*R*)-butenol molecules of 3%. This result is in excellent agreement with the experimental value mentioned.

Concluding remarks

It is clear that the crystal field optimized butenol geometries deviate drastically from the structure typical for an isolated molecule. The differences between the calculated and the experimental geometries of the butenol isomers within the TOT lattice are small and thus acceptable from the experimental point of view. The crystal field *ab initio* approach is clearly capable of dealing with the geometrical influences of packing effects and intermolecular interactions as they occur within the TOT–butenol clathrate. However, our electrostatic concept which ignores attractive/repulsive forces, *e.g.* produced by overlapping electron clouds of adjacent molecules, is not yet reliable enough for cluster energies. The energy difference calculated for isolated butenol molecules in their optimized solid-state geometries confirms the observed chiral discrimination in favour of the TOT–(*R*)-butenol interaction. Our current analysis looks like a welcome addition to the existing tools designed to cope with host–guest interactions in cage compounds.

KV gratefully acknowledges financial support as a predoctoral fellow by the Belgian Organisations IWONL and IWT. CVA thanks the Belgian National Fund for Scientific Research (NFWO) for an appointment as 'Onderzoeksleider'.

References

ALLEN, F. H., KENNARD, O. & TAYLOR, R. (1983). *Acc. Chem. Res.* **16**, 146–153.

ARAD-YELLIN, R., GREEN, B. S., KNOSSOW, M. & TSOUCARIS, G. (1983). *J. Am. Chem. Soc.* **105**, 4561–4571.

GERDIL, R. & ALLEMAND, J. (1980). *Helv. Chim. Acta*, **63**, 1750–1753.

KETELAAR, J. A. A. (1958). *Chemical Constitution*, pp. 35–36. Amsterdam: Elsevier Publishing Company.

KIHARA, T. J. (1960). *J. Phys. Soc. Jpn*, **15**, 1920.

LENSTRA, A. T. H., VAN ALSENOY, C., VERHULST, K. & GEISE, H. J. (1994). *Acta Cryst.* B**50**, 96–106.

PEETERS, A., VAN ALSENOY, C., LENSTRA, A. T. H. & GEISE, H. J. (1994). *J. Mol. Struct. (Theochem.)* **304**, 101–107.

POPELIER, P., LENSTRA, A. T. H., VAN ALSENOY, C. & GEISE, H. J. (1989). *J. Am. Chem. Soc.* **111**, 5658–5660.

POPELIER, P., LENSTRA, A. T. H., VAN ALSENOY, C. & GEISE, H. J. (1991). *Struct. Chem.* **2**, 3–9.

PULAY, P., FOGARASI, G., PANG, F. & BOGGS, J. E. (1979). *J. Am. Chem. Soc.* **101**(10), 2550–2560.

ROGERS, D. (1975). *Anomalous Scattering*, pp. 231–250. Published for the International Union of Crystallography by Munksgaard, Copenhagen.

SIRIPITAYANANON, J. & GERDIL, R. (1989). *Acta Cryst.* C**45**, 768–771.

SMITH, Z., CARBALLO, N., BRIGHT WILSON, E., MARSTOKK, K.-M. & MØLLENDAL, H. (1985). *J. Am. Chem. Soc.* **107**, 1951–1957.

VAN ALSENOY, C. (1988). *J. Comput. Chem.* **9**, 620–626.

VAN ALSENOY, C. & PEETERS, A. (1993). *J. Mol. Struct.* **286**, 19–34.